Arab J Sci Eng (2016) 41:3381–3397
DOI 10.1007/s13369-015-1917-1

RESEARCH ARTICLE - ELECTRICAL ENGINEERING

Optimal Application of Fault Current Limiters for Assuring Overcurrent Relays Coordination with Distributed Generations

A. Elmitwally[1] · **E. Gouda**[1] · **S. Eladawy**[1]

Received: 27 December 2014 / Accepted: 13 October 2015 / Published online: 30 October 2015

Abstract This paper addresses the problem of overcurrent relays (OCRs) coordination in presence of DGs. OCRs are optimally set to work in a coordinated manner to isolate faults with minimal impacts on customers. Penetration of DGs into the power system changes the fault current levels seen by the OCRs. This can deteriorate the coordinated operation of OCRs. Operation time difference between backup and main relays can be below the standard limit or even the backup OCR can incorrectly work before the main OCR. Though resetting of OCRs is tedious especially in large systems, it cannot alone restore the original coordinated operation in the presence of DGs. The paper investigates the optimal utilization of fault current limiters (FCLs) to maintain the directional OCR-coordinated operation without any need to OCRs resetting irrespective of DGs status. It is required to maintain the OCRs coordination at minimum cost of prospective FCLs. Hence, the FCL location and sizing problem are formulated as a constrained multi-objective optimization problem. Multi-objective particle swarm optimization is adopted for solving the optimization problem to determine the optimal locations and sizes of FCLs. The proposed algorithm is applied to meshed and radial power systems at different DGs arrangements using different types of FCLs. Moreover, the OCR coordination problem is studied when the system includes both directional and non-directional OCRs. Comparative analysis of results is provided.

Keywords Overcurrent relay · Coordination · Fault current limiter · Optimization

✉ A. Elmitwally
kelmitwally@yahoo.co.uk

[1] Electrical Engineering Department, Mansoura University, Mansoura 35516, Egypt

List of symbols

A, B, C	Relay characteristic constants
CTI	Coordination time interval for backup–primary relay pair (in s)
i, j	Relay indices
I_{fi}	ith relay near-end-fault current (in A).
$I_{fj,i}$	jth relay fault current for near-end fault at ith relay (in A)
I_{pi}	ith relay pickup current setting (in A)
$I_{pi}\min$, $I_{pi}\min$	Lower and upper limits of I_{pi}
$I_{pi,\text{Fixed}}$	Specific value of I_{pi}
J	Sum of operation time of the primary relays (in s)
LDC	Local distribution company
M_i	ith relay multiple of pickup current
$M_{j,i}$	jth relay multiple of pickup current for the ith relay near-end fault
N	Total number of overcurrent relays in the system N
N_p	Number of backup–primary OCR pairs.
RCTI	Revised coordination time interval for the backup–primary relay pair (in s)
t_i	Operating time of the ith primary relay for near-end fault (in s)
$t_{j,i}$	Operating time of the jth backup relay for near-end fault at the ith primary relay (in s)
Δt	operating time difference $= t_{j,i} - t_i$
TDS_i	Time dial setting for the ith relay
$\text{TDS}_{i\,\min}$, $\text{TDS}_{i\max}$	Lower and upper limits of TDS_i
FCL	Fault current limiter
R-FCL	Resistive fault current limiter

X-FCL	Inductive fault current limiter
Z-FCL	Resistive–inductive fault current limiter
$t_{B,bDG}$	Operating time of backup relay before DG
$t_{M,bDG}$	Operating time of main relay before DG
$t_{B,aDG}$	Operating time of backup relay after DG
$t_{M,aDG}$	Operating time of main relay after DG
R_i	Resistance of the ith FCL
X_i	Inductive reactance of the ith FCL
L	Number of FCLs
R_{min}, and R_{max}	Lower and upper limits of FCL resistance
X_{min}, and X_{max}	Lower and upper limits of FCL inductive reactance

1 Introduction

Integration of distributed generation (DG) can improve reliability, reduce power losses, improve power quality, decrease environmental pollution, and diminish the need for network expansions. The protection devices are set to have a coordinated operation. This enables to isolate faults with minimum impact on customers. When DG units are connected to a distribution network, the magnitude and direction of fault current will change. So, the coordination between the network protection devices may vanish [1]. Autorecloser-fuse miscoordination and relay–relay miscoordination can occur. Size of DG, location of DG, and type of DG (static or rotating machine) influence the share of DG in total fault current. Thus, these factors determine the DG effect on protection system coordination [2]. Directional overcurrent relays (DOCRs) form the primary protection of distribution and sub-transmission systems and the secondary protection of transmission systems. The coordination of overcurrent relays (OCRs) is realized by adjusting the pickup current setting (I_p) and the time dial setting (TDS) of each OCR to maximize the selectivity and reliability of the protective system [3]. Setting of OCRs is difficult, especially in the multi-loop, multi-source networks. Trial-and-error, topological analysis, and optimization methods are used for OCRs setting [4].

Possible solutions to the OCRs miscoordination problem in power delivery system (PDS), with and without DGs, are searched in literature [5–13]. In case of PDS without DG, the authors in [5] reported a systematic approach for OCRs coordination by breaking all system loops. In [6,7], a linear graph theory-based method was used for OCRs coordination. Furthermore, optimization techniques such as dual simplex [8,9] and genetic algorithms [10] were used to minimize the relay operating times. To provide coordination between OCRs in the presence of DG, Ref. [11] discussed high-impedance protection applications for tripping acceleration. But this method depends on current transformer (CT) whose dynamic behavior influences the protection stability. Ref. [12] proposes the use of distribution system automation capabilities for protection coordination. One drawback of this method is that the number of protection zones increases with the increase in number of DGs. So, many isolating circuit breakers will be needed and the scheme may not be economic. Communication-assisted digital relay approach is presented in [13] to achieve coordinated operation of OCRs. Complexity and enlarged failure rates are major concerns in this method.

One approach to control fault current with DG is the use of fault current limiter (FCL) [14]. FCL basically provides nearly zero impedance in normal operation without energy loss or voltage drop. If a fault occurs, the FCL will insert high impedance in the current path within few milliseconds to reduce the fault currents to lower levels [14]. FCLs can be divided into three main categories [15]: passive FCLs, solid-state FCLs, and hybrid FCLs. Passive FCLs insert a current-limiting inductance without external control signals. The solid-state FCL is formed by utilizing power electronics equipment and sensors. Hybrid FCLs use combination of mechanical switches, solid-state devices, superconducting materials and other technologies to mitigate fault current [15]. FCLs are generally sophisticated and expensive equipment. FCL size may be defined as the impedance value it introduces under fault conditions. The FCL cost gets higher as its size increases. Placement and sizing of FCLs in a power network greatly determine its impact on protection system. To minimize the total cost of protective devices, genetic algorithm-based method was implemented to determine the optimal locations of FCLs in a radial distribution system with DG in [16]. Although the optimal FCLs sizes for a distribution system with DG are determined mathematically in [17], the FCL locations are hypothetically assumed, and their cost is not considered. In [18], FCLs are utilized to restore DOCR coordination in the presence of DG. The optimal DOCR settings without DG are maintained under DG. This avoids any need to DOCR resetting. However, sizes and locations of FCLs are estimated by trial-and-error method and cannot be optimal from performance and cost perspectives.

In this paper, optimally allocated FCLs are used to restore the coordination of OCRs in PDS with DG. The FCL allocation problem involves more than one objective function such as level of fault current damping and FCLs sizes. These objectives are contradictory and of different dimensions. So, the problem is formulated as a multi-objective constrained nonlinear programming problem. The interaction among different objectives yields a set of compromised solutions, largely known as the trade-off, non-dominated, or Pareto-optimal solutions [19]. The optimization problem is solved using particle swarm optimization (PSO).

The novel aspects of this paper are:

1. Propose an index for the coordination of the main–backup OCR pairs in presence of DGs.
2. Present a new multi-objective formulation of the OCRs coordination maintenance problem in power systems with DGs by FCLs. The model considers the OCRs coordination and the FCLs sizes (cost) as two conflicting objectives to be optimized.
3. Search both optimal locations and sizes of FCLs with no pre-assumptions.
4. Consider the application of FCLs in a mixed system of both directional and non-directional OCRs in presence of DGs.
5. Compare the OCRs coordination and coordination maintenance problems in looped and radial networks.
6. Compare the performance of three different FCL types.

2 Proposed Relay Coordination Restoration Approach

2.1 Determination of the Original Relay Coordination

The time dial setting defines the operation time (t) of the OCR for each relay current value (I). M is the current multiple of the pickup current value, i.e., $M = I/I_p$. t is normally given as a function of M based on the OCR characteristics. The IEEE OCR characteristics are adopted in this work and are given as [20–22]:

$$t_i = \mathrm{TDS}_i \left(\frac{A}{M_i^C - 1} + B \right) \quad \text{with} \quad M_i = \frac{I_{fi}}{I_{pi}} \tag{1}$$

$$t_{j,i} = \mathrm{TDS}_{j,i} \left(\frac{A}{M_{j,i}^C - 1} + B \right) \quad \text{with} \quad M_{j,i} = \frac{I_{fj,i}}{I_{pj}} \tag{2}$$

The primary objective of the OCR coordination problem is to minimize the sum of operation time of the primary OCRs as given by (3).

$$\text{Minimize} J = \sum_{i=1}^{N} t_i \tag{3}$$

Time dial setting and pickup current setting are determined for each relay provided that certain coordination constraints are met [20]. For this purpose, a two-phase optimization model is mathematically formulated in (3)–(9) [18]. In Phase 1, the objective J given in (3) is minimized subject to the set of constraints given in (4)–(6). In Phase 2, the objective J given in (3) is minimized subject to another set of constraints given in (7)–(9) to further tune the OCR setting determined in Phase 1.

(i) For Phase 1
There are relay setting constraints as in (4), (5) and backup–primary OCR pairs (BMOP) constraints as in (6) [21].

$$I_{pi\,\min} \le I_{pi} \le I_{pi\,\max} \tag{4}$$

$$\mathrm{TDS}_{i\,\min} \le \mathrm{TDS}_i \le \mathrm{TDS}_{i\,\max} \tag{5}$$

$$t_{j,i} - t_i \ge \mathrm{CTI} \tag{6}$$

The backup OCR should not operate until the primary OCR fails to operate. But, if the backup OCR is needed to operate, it should wait for a minimum time interval of CTI after the assumed operating time of the primary OCR [23]. The value of CTI is chosen based on the LDC practice. It accounts for relay operating time, the breaker operating time, and safety margin for relay error.

(ii) For Phase 2
I_{pi} determined in Phase 1 is approximated to the nearest standard value and kept fixed during the search process. CTI is modified to a lower practical value RCTI that is typically 90 % of CTI [20].

$$I_{pi} = I_{pi,\mathrm{Fixed}} \tag{7}$$

$$\mathrm{TDS}_{i\,\min} \le \mathrm{TDS}_i \le \mathrm{TDS}_{i\,\max} \tag{8}$$

$$t_{j,i} - t_i \ge \mathrm{RCTI} \tag{9}$$

The optimization problem formed by (3) and (7)–(9) is solved to get the final TDS settings of the OCRs.

2.2 Restoration of the Original Relay Coordination

The BMOP coordination determined above without DGs can deteriorate by integrating DGs to the system. To maintain the original OCRs coordinated settings in presence of DGs, it is proposed to use optimally allocated FCLs. The set of required FCLs impedance values is a function of DG capacity, number of DGs, and DGs locations [21]. To keep the original OCRs settings obtained above unchanged, the prospective optimal FCLs must keep almost the same OCR fault current before DG integration. Therefore, the same OCRs operating times are kept in presence of DGs. This in turn maintains the desired original coordinated operation of BMOP irrespective of DGs status.

3 Problem Formulation

It is assumed that BMOP are properly set to assure coordinated operation in a DG-free PDS. Integration of DGs will feed additional fault current that may lead to loss of coordination of OCRs. Thus, the main objective of this paper is to

minimize such change in the OCR-seen fault current levels by optimal placement and sizing of FCLs. This keeps the coordinated operation of BMOP. The coordination index of BMOP (RPCI) is proposed as:

$$\text{RPCI} = \sum_{n=1}^{N_p} \text{abs}\left(\left(t_{\text{B,bDG}} - t_{\text{M,bDG}}\right) - \left(t_{\text{B,aDG}} - t_{\text{M,aDG}}\right)\right)_n \tag{10}$$

The ideal value of RPCI is zero as it means perfect coordination between BMOP under DGs.

The FCL-based BMOP coordination maintaining problem is formulated as multi-objective constrained nonlinear optimization problem.

Objective functions:

$$\text{Min } F1 = \text{RPCI} \tag{11}$$

$$\text{Min } F2 = \sum_{k=1}^{L} R_k + X_k \tag{12}$$

The above problem is solved subject to the following inequality constraints:

$$R_{\min} \le R_i \le R_{\max} \tag{13}$$

$$X_{\min} \le X_i \le X_{\max} \tag{14}$$

$$t_{\text{B,aDG}} - t_{\text{M,aDG}} > \text{RCTI} \tag{15}$$

4 Solution Algorithm

The maximum number of FCLs to be connected to the system equals the sum of number of lines and number of power sources. Particle swarm optimization (PSO) is presented recently as an efficient heuristic search method to obtain the global or quasi-global optimal solution in power system optimization problems [21,22]. Single-objective PSO searches the minimum or maximum value of a single-objective function. Multi-objective PSO (MOPSO) searches the minimum values of multiple objectives simultaneously. Since these objectives can be conflicting, the problem has a set of candidate compromised solutions rather than a single solution. This set of different solutions is known as the Pareto-optimal set. Three main issues are considered on implementing MOPSO [22]. These include giving preference to non-dominated solutions, retaining the non-dominated solutions found during the search process, and maintaining diversity in the swarm. MOPSO is well explained in [23,24]. It is employed to solve the optimization problem formulated in (11)–(15). The solution algorithm is implemented as given below.

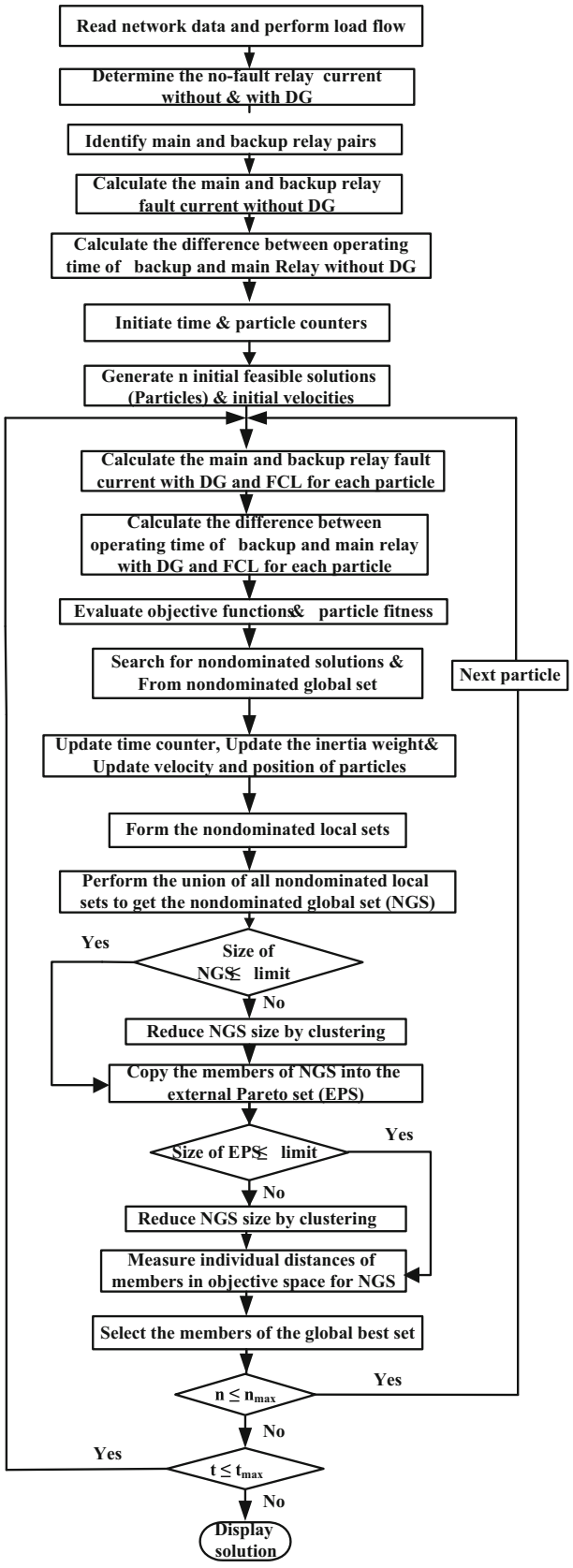

Fig. 1 Flowchart of restoring OCRs coordination using optimal FCLs

1. Disconnect all DGs, apply a solid symmetrical three-phase fault at the nearest bus to each main OCR (one at a time), the short-circuit currents seen by this OCR and its backup OCRs are calculated. Estimate the operation time of each BMOP from (1) and (2).
2. Set the time counter $t = 0$ and generate randomly $n$particles, $\{Xj(0), j=1, \ldots, n\}$. Similarly, generate randomly initial velocities of all particles, $\{Vj(0), j=1, \ldots, n\}$. Each particle includes values for all control variables to be optimized, resistance and inductance for each possible FCL. Set the initial value of the inertia weight.
3. Connect all DGs. Insert the FCLs estimated by a particle (possible set of FCLs). Apply a solid symmetrical three-phase fault at the nearest bus to each main OCR (one at a time), the short circuit currents seen by this OCR and its backup OCRs are calculated. Estimate the operation time of each BMOP from (1) and (2). Repeat for all particles.
4. Calculate the objectives F1, F2 values for each particle using (11) and (12). Then, compute the fitness value of each particle as:

$$\text{Fitness} = 1/\sum_{i=1}^{Q} w_i F_i \tag{16}$$

where, w_i is a weighting factor such that $\sum w_i = 1$. F_i is the value of the ith objective function. Q is the number of objective functions.

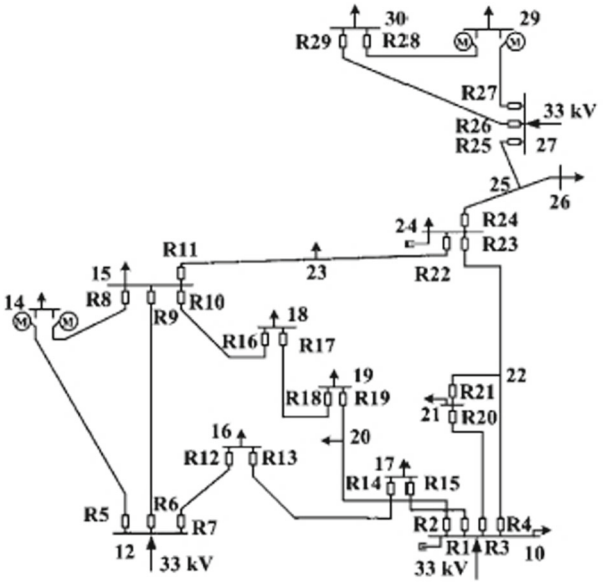

Fig. 2 Meshed system under study

Table 1 Main and backup relay in the meshed system

Main relay	Backup relay	Main relay	Backup relay
1	19, 23	15	13
2	15, 23	16	18
3	15, 19, 23	17	10
4	15, 19, 23	18	2
5	9, 12	19	17
6	8, 12	20	4, 23
7	8, 9	21	3, 4, 23
8	6, 12	22	4, 25
9	5, 16	23	11, 25
10	5, 6	24	4, 11
11	5, 6, 16	25	24, 29
12	14	26	24
13	7	27	24
14	1	28	26, 27
		29	27

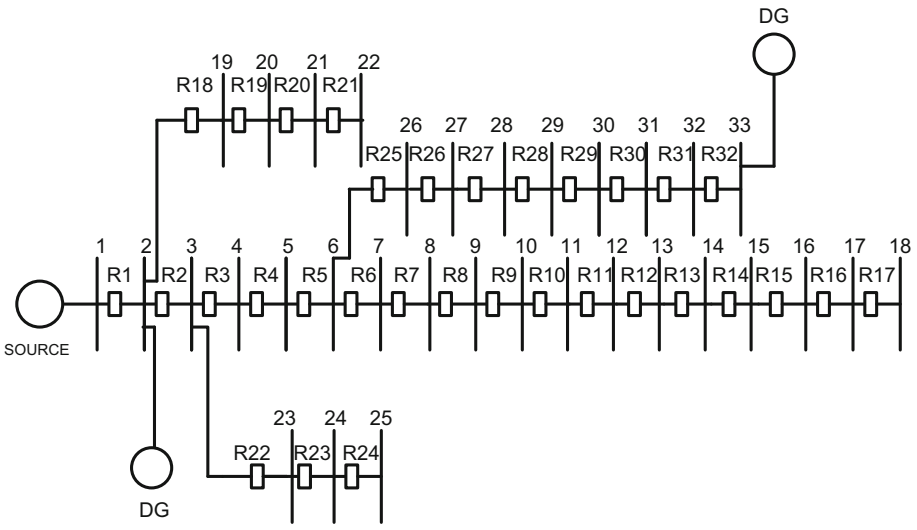

Fig. 3 IEEE 33-bus radial system

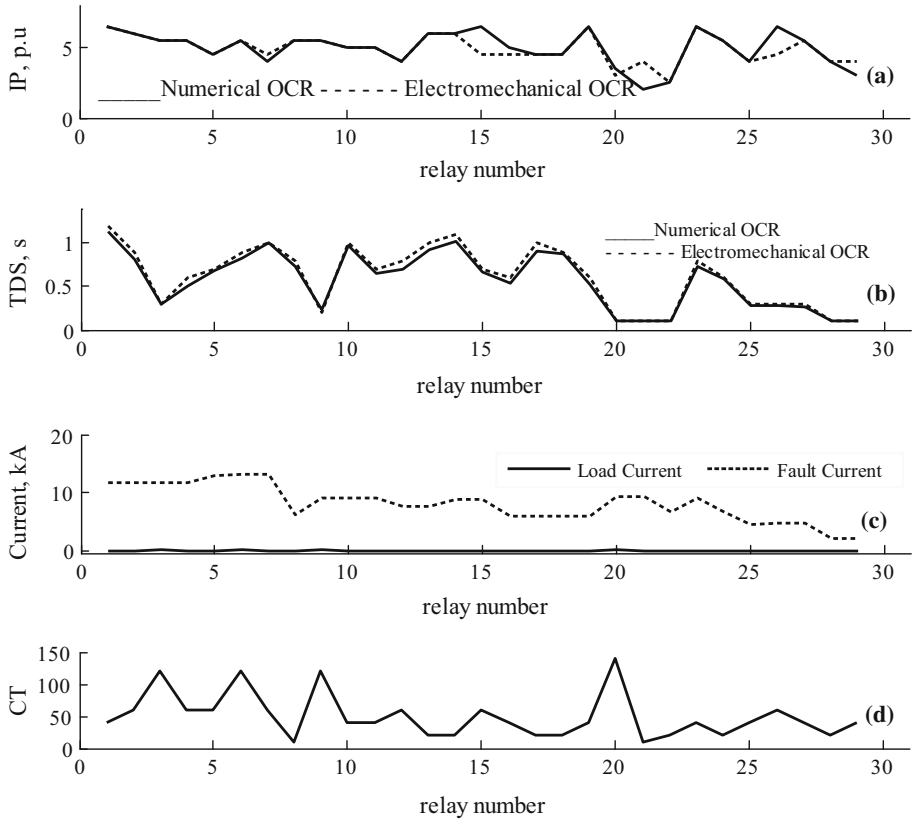

Fig. 4 Optimal settings for primary DOCRs in meshed system. **a** The pickup current(I_p, p.u), **b** the time dial setting (TDS, s), **c** the normal load and fault currents, **d** the current transformer ratio

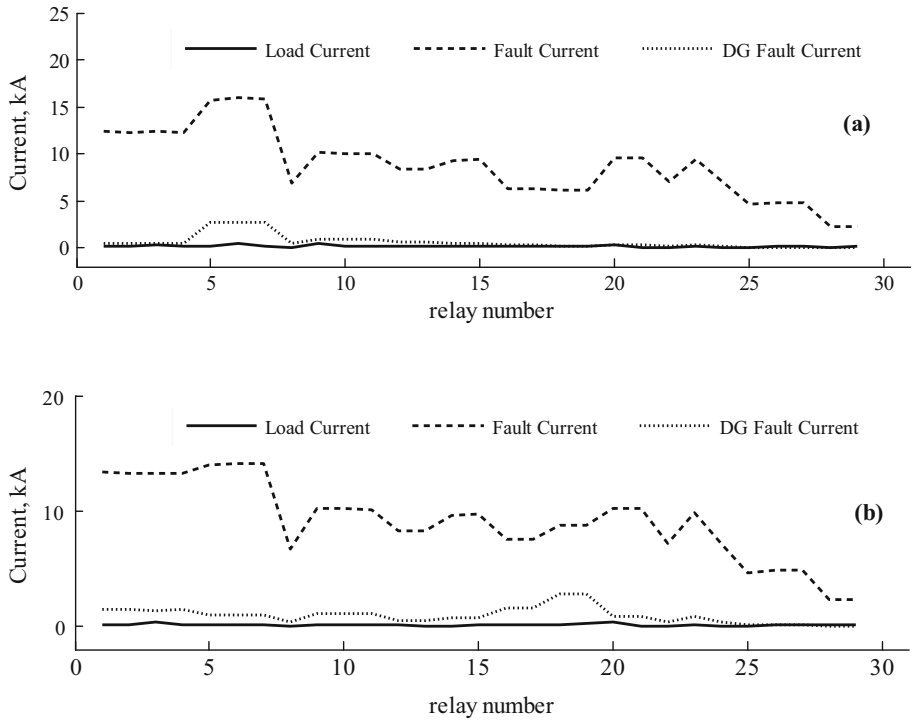

Fig. 5 Samples of normal load relay current, near-end- fault relay current, and DG-supplied fault current in the meshed system **a** DG at bus 12, **b** DG at bus 19

5. Search for the non-dominated solutions and form the non-dominated global set $S^{**}(0)$. The best member in $S^{**}(0)$ is selected as the global best $Xj^{**}(0)$. Set the external set equal to $S^{**}(0)$.
6. Update the time counter $t = t + 1$.
7. Update the inertia weight.
8. Update the particle velocity and position.

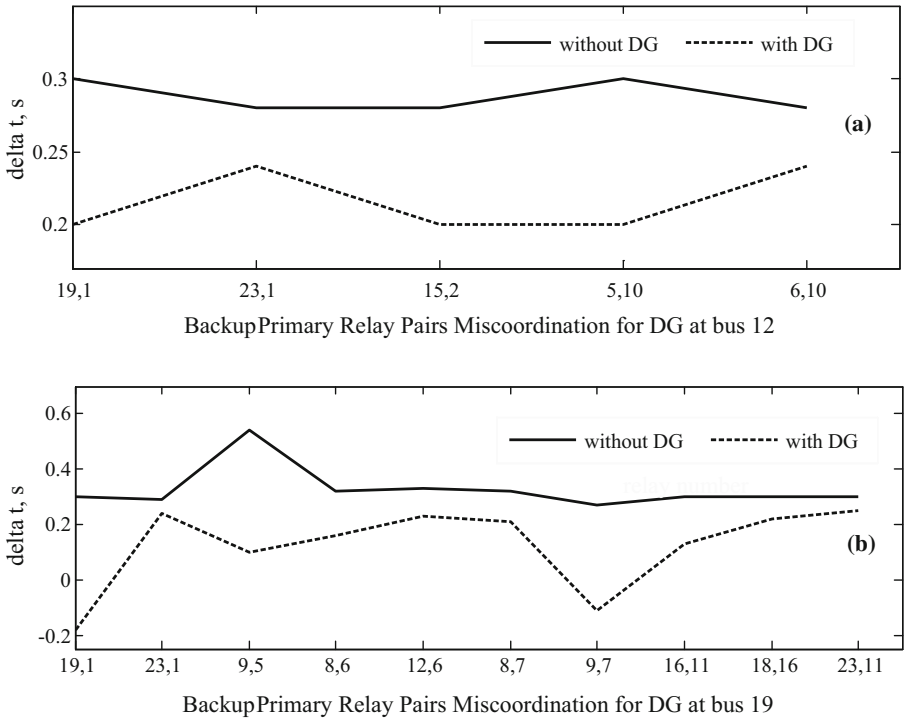

Fig. 6 BMOP miscoordination in the meshed system **a** for DG at bus 12, **b** for DG at bus 19

9. The updated position of the jth particle is added to $Sj^*(t)$. Truncate the dominated solutions in $Sj^*(t)$. If the size of $Sj^*(t)$ exceeds a prespecified value, reduce the size to its maximum limit by the hierarchical clustering algorithm [23].
10. Perform the union of all non-dominated local sets to produce the non-dominated global set $S^{**}(t)$. If the size of $S^{**}(t)$ exceeds a maximum limit, reduce this set size by hierarchical clustering algorithm.
11. Copy the members of $S^{**}(t)$ to the external Pareto set. If the number of the Pareto set members exceeds the maximum size, reduce the set by means of clustering.
12. Measure the individual distances between members in $Sj^*(t)$, and members in $S^{**}(t)$ in the objective space. The members of $Sj^*(t)$ and $S^{**}(t)$ that give the minimum distance are selected as the local best and the global best, respectively.
13. If the termination criterion is met, then stop. Else go to step 3.

Flowchart of restoring OCRs coordination using optimal FCLs is shown in Fig. 1.

5 Results and Discussion

A meshed system and a radial system are analyzed in this work. The meshed system under study is a part of the IEEE 30-bus system [25] depicted in Fig. 2. This PDS is assumed to

Table 2 Number of relay pair miscoordination

DG location	Δt < RCTI	Backup relay operates before primary relay
Bus10	0	6
Bus12	0	5
Bus15	2	8
Bus16	0	6
Bus17	0	6
Bus18	2	7
Bus19	2	8
Bus21	0	5
Bus24	1	8
Bus27	0	3
Bus30	0	3

Table 3 Determined FCLs for DG at buses 12, 19

FCL location (in series to)	X-FCL size (p.u)
Source at bus1	1.858
DG at bus12	10
DG at bus19	10
Source at bus5	2.469
Source at bus13	0.014
Objective function F1	1.263
Sum of FCLs components sizes (p.u.)	24.5

Table 4 Determined FCLs for three DGs at buses 10, 12, 19

FCL location (in series to)	FCL size (p.u)		
	X-FCL	R-FCL	Z-FCL
Source at bus1	3.769	0	1
Source at bus2	0	0	0.5
DG at bus10	0	4.092	$1.5 + j3$
DG at bus12	4.970	0	0
DG at bus19	10	2.243	$1.5 + j1$
Source at bus5	0.309	0	$3.8 + j1.8$
Source at bus8	0	0.022	$1.4 + j1.10$
Source at bus11	0	4.942	$3.2 + j1.7$
Source at bus13	0	9	$2.8 + j2.7$
Objective function F1	0.160	2.215	2.8
Sum of FCLs components sizes (p.u.)	19.210	20.301	26.6

Table 5 X-FCLs determined in [18]

FCL location (in series to)	Two DGs at buses 12, 19		Three DGs at buses 10, 12, and 19		
	DG at bus 12	DG at bus 19	DG at bus 10	DG at bus 12	DG at bus 19
X-FCL size (p.u.)	56	56	42	42	42
Sum of X-FCL sizes (p.u.)	112		126		
Δt (R1, R19)	0.2702		0.2709		

Table 6 R-FCLs determined in [18]

FCL location (in series to)	Two DGs at buses 12, 19		Three DGs at buses 10, 12, and 19		
	DG at bus 12	DG at bus 19	DG at bus 10	DG at bus 12	DG at bus 19
R-FCL size (p.u.)	22	22	18	18	18
Sum of R-FCL sizes (p.u.)	44		54		
Δt (R1, R19)	0.2711		0.2746		

have 29 DOCRs. The radial system is the IEEE 33-bus radial distribution system shown in Fig. 3. These test system data are provided in [26]. It has 33 DOCRs located as depicted in Fig. 3. It is assumed that all relays are identical and have the standard IEEE relay curves with the constants values of 0.0515, 0.114, and 0.02 for A, B, and C,, respectively, [27]. OCRs are assumed to be optimally set and well coordinated before DG integration. CTI is assumed to be 0.3 s for each backup–primary OCR pair. The chosen DG technology is a synchronous-type, operating nominally at 0.9 lagging power factor, and has a 0.15 p.u transient reactance based on its capacity. The DG is practically connected to the PDS bus through a transformer with 0.05 p.u reactance based on its capacity [28].

5.1 Meshed System

Three scenarios are examined to evaluate the effectiveness of utilizing FCLs to restore the original OCR coordination for the meshed PDS with DGs.

(i) Scenario A: It is the base case with well-established OCR coordination, where there is no DG in the PDS.
(ii) Scenario B: DG is presented. It is the worst case as BMOP miscoordination arises.
(iii) Scenario C: It illustrates the proposed approach of installing optimally allocated FCLs to restore the BMOP coordination.

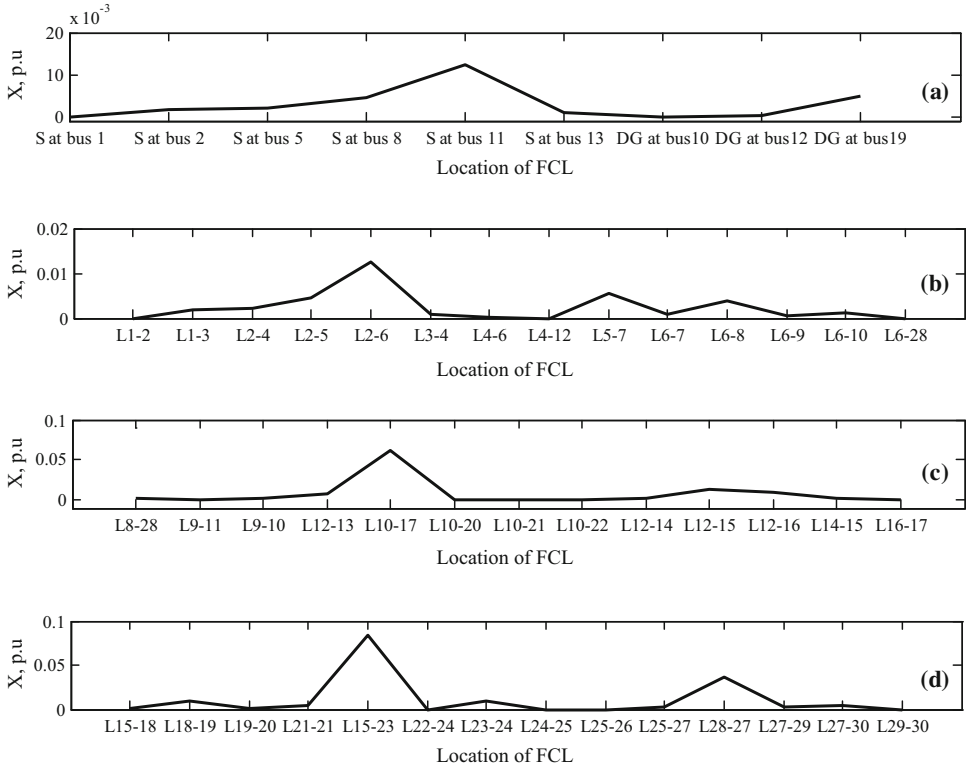

Fig. 7 Determined X-FCLs for three DGs in the meshed test system

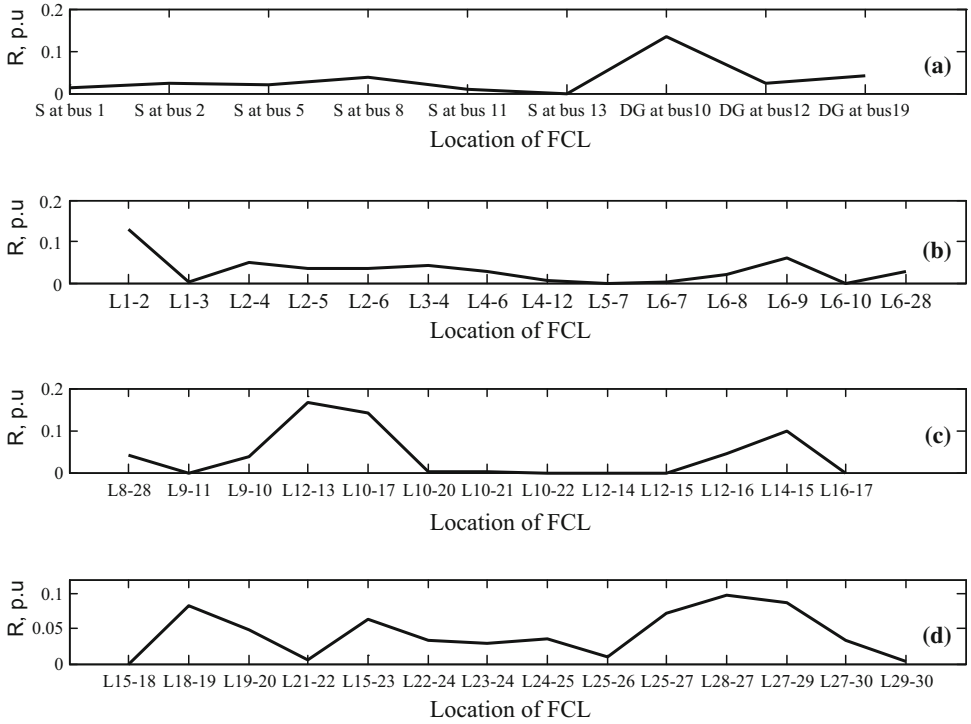

Fig. 8 Determined R-FCLs for three DGs in the meshed test system

5.1.1 Scenario A: BMOP Coordination Without DGs

Each OCR represents a main protection and has other OCRs serving as a backup protection. So, Table 1 defines backup OCRs for each relay in the meshed system [19].

The two-phase DOCR optimal setting process discussed in Sect. 2 is carried out using GAMS software [29]. The minimum and maximum I_p limits are chosen to be 1.25 and 2 times the maximum no-fault current seen by each OCR, respectively. On the other hand, the minimum TDS

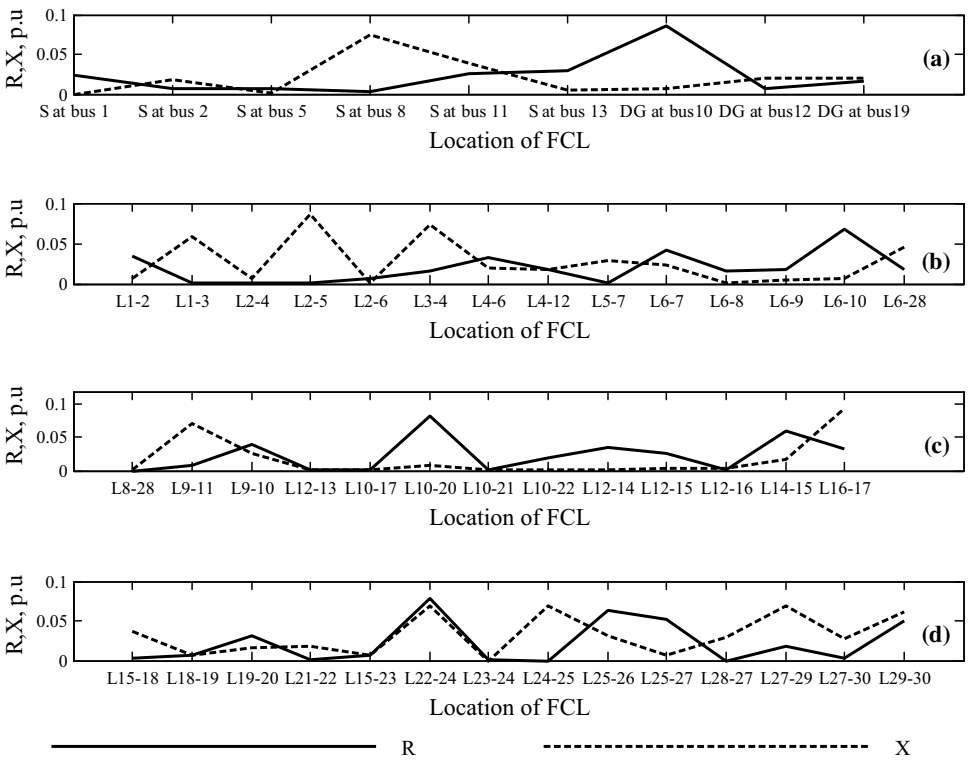

Fig. 9 Determined Z-FCLs for three DGs in the meshed test system

Table 7 Δt of selected backup–primary relay pairs

DOCR pair	No DG	3 DGs and no FCL	3 DGs and X-FCL
19, 1	0.368	0.046	0.605
8, 6	0.288	0.228	0.800
8, 7	0.319	0.256	0.292
9, 7	0.326	0.086	0.520
16, 11	0.275	0.193	0.338

Table 8 Main and backup relay for IEEE 33-bus radial system

Main relay	Backup relay	Main relay	Backup relay
2	1	17	16
3	2	18	1
4	3	19	18
5	4	20	19
6	5	21	20
7	6	22	2
8	7	23	22
9	8	24	23
10	9	25	5
11	10	26	25
12	11	27	26
13	12	28	27
14	13	29	28
15	14	30	29
16	15	31	30
		32	31

is assumed to be 0.1 s in all cases. The obtained relays I_p are rounded and kept fixed at the nearest standard setting [27].

Rounding the I_p results obtained in Phase 1, CTI constraints in (4) are violated for 15 pairs out of the 51 BMOP. The chosen RCTI values are 0.284 and 0.27 s for numerical and electromechanical OCRs, respectively. After conducting Phase 2 of OCR optimal setting given in (3) and (7)–(9) using GAMS, the obtained rounded Ip and TDS settings satisfy the constraints (7)–(9) for all OCRs. Figure 4 shows the optimal settings of the DOCRs in the meshed system.

5.1.2 Scenario B: Relay Coordination in Presence of DG

DG changes the value of fault current, and it may bring BMOP miscoordination. Figure 5 reports samples of relay normal load current, near-end-fault current, and DG-supplied fault current in the meshed system for single-DG operation at bus 12 and at bus 19. For DG at bus 12, miscoordination occurs for five BMOP, based on RCTI threshold (0.27 s). Figure 6a compares Δt of related BMOP in the meshed system with and without DG for a DG installed at bus 12. It is clear

Table 9 FCLs obtained by single objective for IEEE 33-bus radial system

FCL location (in series to)	Size (p.u)		
	Z-FCL	X-FCL	R-FCL
Source at bus1	$1.55 + j0$	1.81	1.53
DG at bus2	$5.67 + j9.49$	20	16.67
DG at bus33	$10 + j10$	20	20
F1 (s)	2.99	3.41	2.79
Sum of FCLs components sizes (p.u.)	36.72	41.81	38.21

that Δt is reduced in case of the presence of DG. In Fig. 6b, BMOP miscoordinations in the meshed system are reported for a DG installed at bus 19. Eight BMOPs (23, 1 & 9, 5 & 8, 6 & 12, 6 & 8, 7 & 16, 11 & 18, 16 & 11, 23) have lower (Δt) than RCTI. Backup relay operates before the primary one for other two pairs (19, 1 & 9, 7). For one DG at buses(10, 12, 15, 16, 17, 18, 19, 21, 24, 27, 30), Table 2 shows the number of BMOP miscoordinations in the meshed system for each DG location, due to either low Δt or backup operation before primary relays. This BMOP miscoordination problem is solved by using FCL as in Scenario C below.

5.1.3 Restoration of DOCR Coordination by FCLs

1. Single-objective function

For two 10-MVA DG units connected to buses 12 and 19 in the PDS of Fig. 2, many BMOP miscoordinations occur. Optimal FCLs to restore coordination are determined firstly by solving the optimization problem discussed in Sect. 3 considering only a single objective in (11). Table 3 shows the minimum X-FCLs sizes and locations required to restore coordination for all BMOP. The sum of obtained minimum X-FCL sizes is 24.5 p.u. Further, for three 10-MVA DGs at buses 10, 12, and 19, the FCL results are given in Table 4 for X-FCL, R-FCL, and Z-FCL types. The choice of the proper FCL type depends on operators experience and FCL type's cost. The results obtained by the proposed method in Tables 3 and 4 are compared to those obtained in [18] and given in Tables 5 and 6. It is remarked that the proposed method, even for single objective, results in coordinating all BMOP at much lower size/cost of the required FCLs for all DG conditions. This may be attributed to that the locations of FCLs are assumed empirically in [18], whereas the proposed method identifies the optimal sizes and locations of FCLs.

2. Multi-objective function

MOPSO is used to solve the full multi-objective FCL allocation problem formulated in (11)–(15) for the meshed test system. Three 10-MVA DG units are connected at buses 10, 12, and 19 in the PDS shown in Fig. 2. Figures 7, 8, and 9 give the determined optimal X-FCLs, R-FCLs, and Z-FCLs,

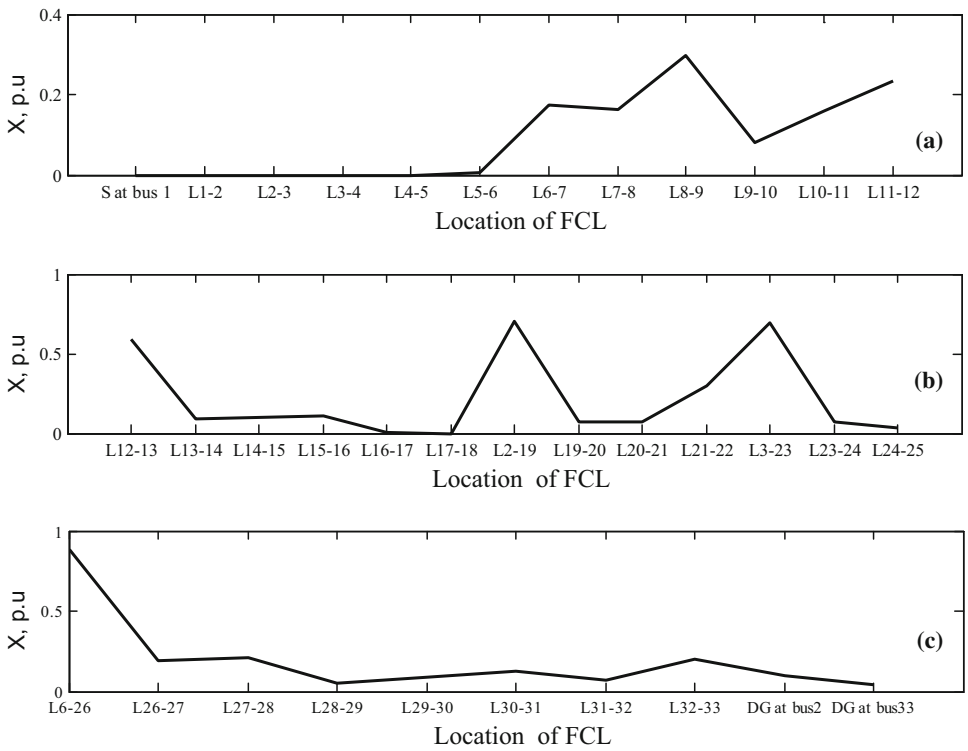

Fig. 10 Determined X-FCLs for two DGs in IEEE 33-bus radial system

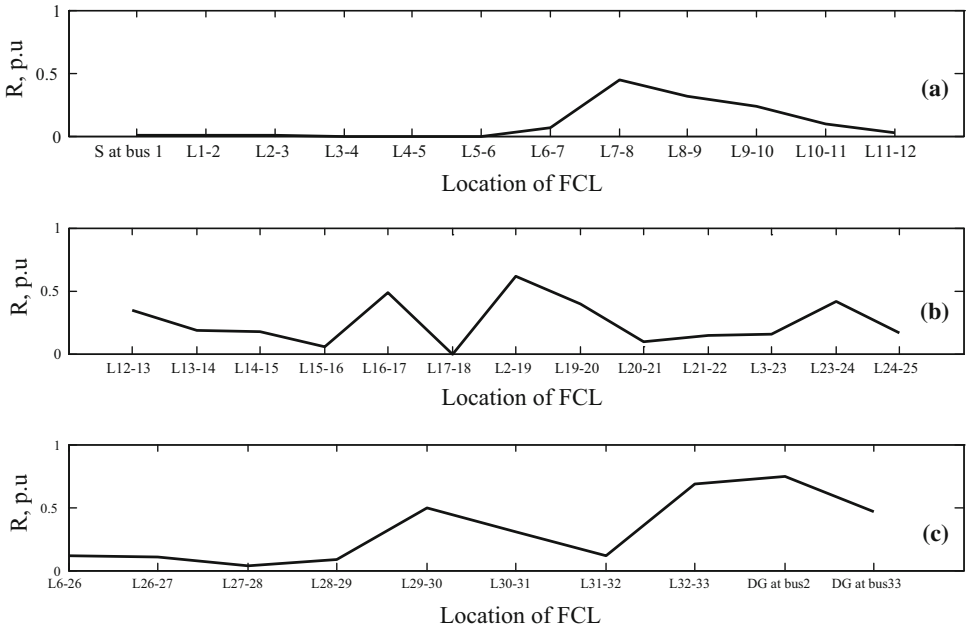

Fig. 11 Determined R-FCLs for two DGs in IEEE 33-bus radial system

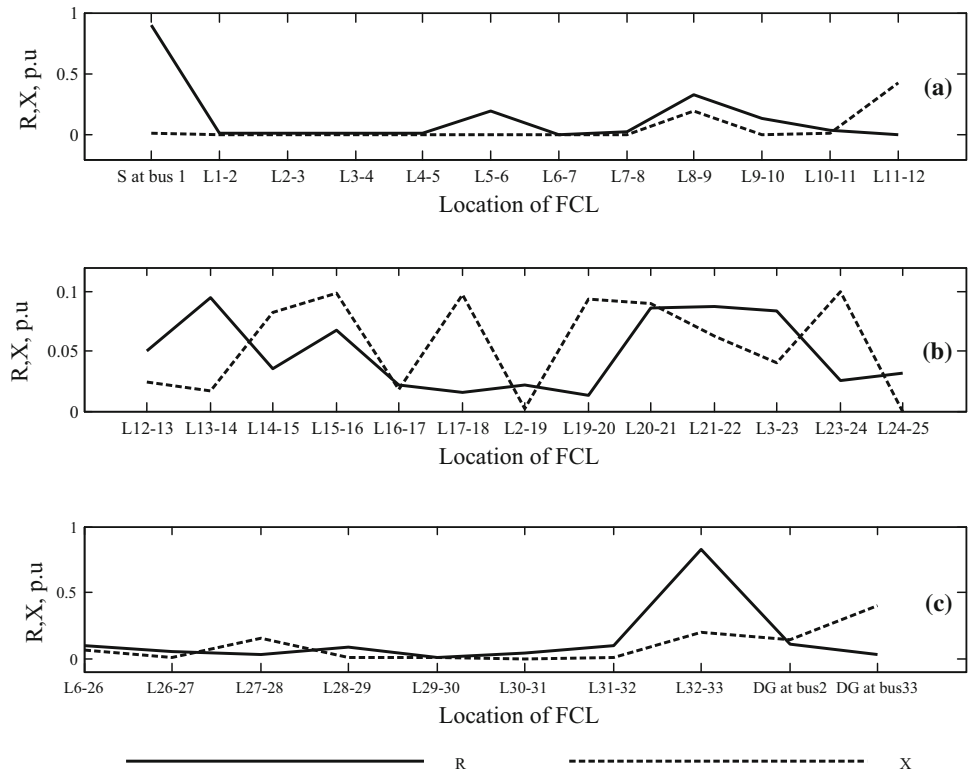

Fig. 12 Determined Z-FCLs for two DGs in IEEE 33-bus radial system

respectively. For the three FCLs types, coordination is maintained for all BMOP after DG integration. The optimal value of (F1) is 1.5, 0.04, and 1.7 s for X-FCLs, R-FCLs, and Z-FCLs, respectively. The sum of required FCLs components sizes (F2) is 0.294, 1.85, and 2.3 p.u. for X-FCLs, R-FCLs, and Z-FCLs, respectively. It is clearly less than obtained by

Table 10 Δt of selected BMOP in IEEE 33-bus radial system

Backup–main OCR pair	$t_{\text{backuprelay}} - t_{\text{mainrelay}}$		
	No DG	DG and no FCL	DG and FCL
6, 7	0.3003	0.2480	0.2731
7, 8	0.3006	0.2580	0.2939
9, 10	0.2993	0.2676	0.2911
10, 11	0.2970	0.2743	0.2912
11, 12	0.2704	0.2308	0.2728
12, 13	0.2708	0.2593	0.2742
13, 14	0.2945	0.2700	0.2953

single-objective optimization or the method in [18]. Table 7 indicates Δt of selected BMOP for various scenarios. Marked cells in Table 7 refer to miscoordination case.

5.2 IEEE 33-Bus Radial Distribution System

BMOP are listed in Table 8. Two 10-MVA DG units are connected at buses 2 and 33 as revealed in Fig. 3.

1. Single-objective function

Table 9 presents the determined optimal X-FCLs, R-FCLs, and Z-FCLs for only single-objective function RPCI in (11).

2. Multi-objective functions

Figures 10, 11, and 12 give the determined optimal X-FCLs, R-FCLs, and Z-FCLs, respectively. For the three FCLs types, coordination is maintained for all BMOP after DG integration. The optimal value of ($F1$) is 2.1, 1.7 and 3.02 s for X-FCLs, R-FCLs, and Z-FCLs, respectively. The sum of required FCLs sizes ($F2$) are 5.9, 7.5, and 6.07 p.u. for X-FCLs, R-FCLs, and Z-FCLs, respectively. FCLs sizes obtained by multiple objective optimization are clearly less than obtained by single-objective optimization. Table 10 indicates Δt of selected BMOP for various scenarios using X-FCLs. Insertion of X-FCLs enables to make Δt above 0.27 s (RCTI) to assure coordination of all BMOP as indicated in Table 10. It is noted that FCLs sizes are much bigger for radial system compared to meshed system.

5.3 Mix of Directional and Non-directional OCRs

For the meshed system in Fig. 2, if the OCRs 1, 5, 16, and 29 are replaced by non-directional OCRs, the primary–backup relay pairs change. Figure 13 reveals the new primary–backup relay pairs. Main relays are set on the x-axis. Corresponding backup ones are shown by bars. Using the same data and method in Sect. 5.A above, Fig. 14 illustrates the obtained final optimal settings of OCRs for this case.

For three 10-MVA DGs at buses 10, 12, and 19, the optimal FCLs are determined by solving the optimization problem in

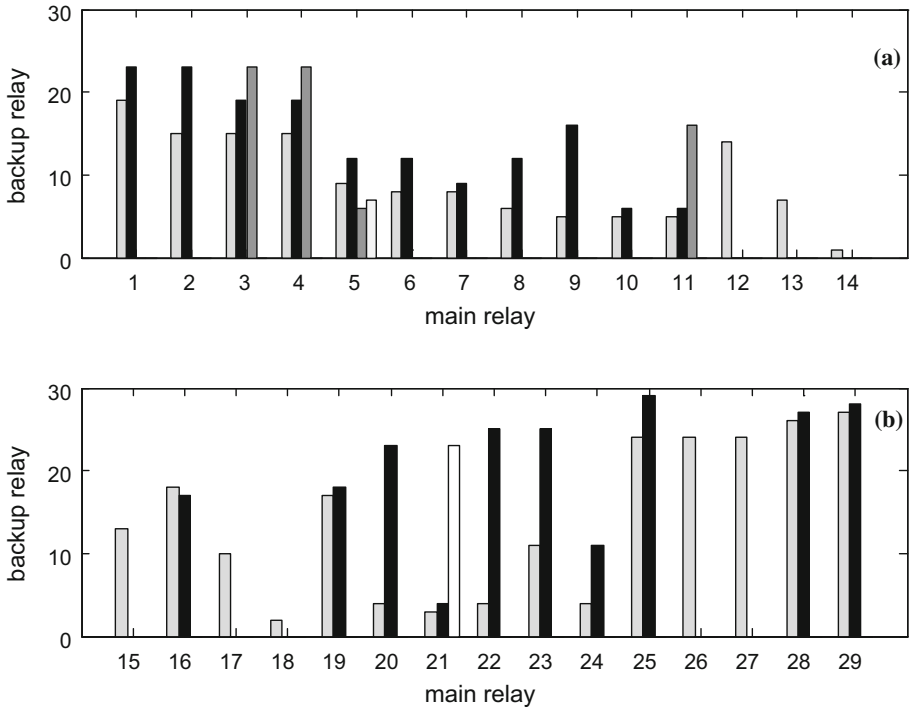

Fig. 13 Primary–backup relay pairs for mixed directional and non-directional OCRs

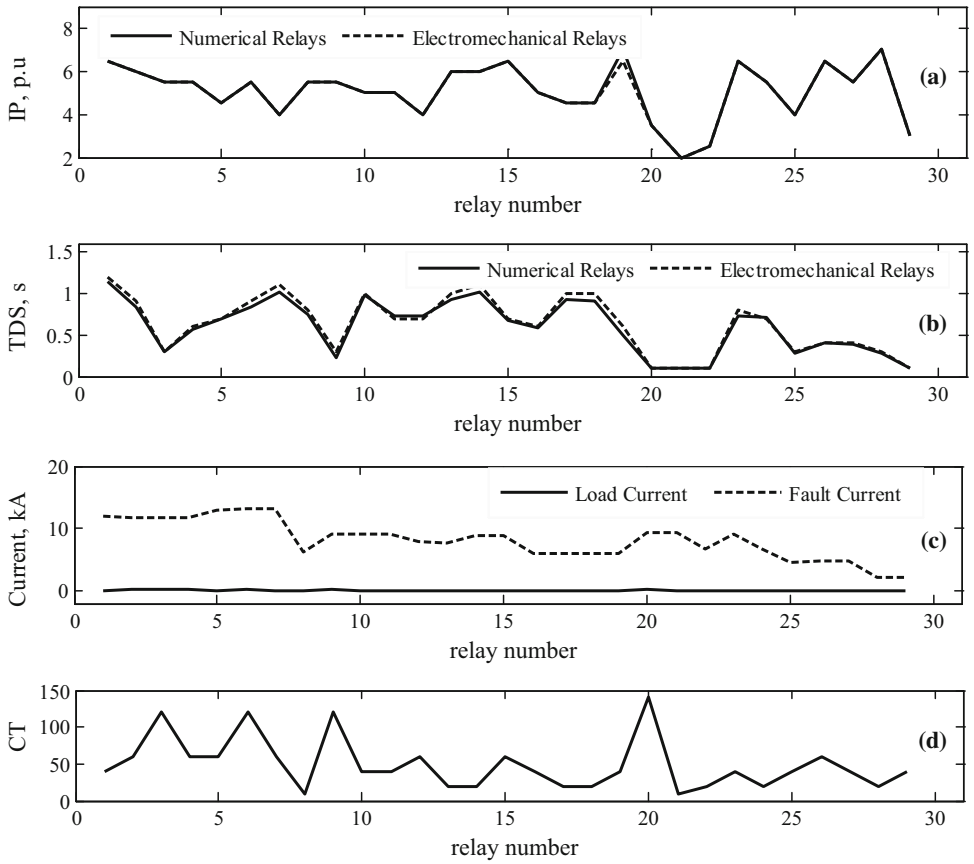

Fig. 14 Optimal settings of primary relays for mixed directional and non-directional OCRs. **a** The pickup current (I_p, p.u), **b** the time dial setting (TDS, s). **c** the normal load and fault currents, **d** the current transformer ratio

Table 11 Determined FCLs for 3 DGs at buses 10, 12, 19 with mixed OCRs (single objective)

FCL location (in series to)	FCL size, p.u		
	X-FCL	R-FCL	Z-FCL
Source at bus1	2.769	1	$0.08 + j0.08$
Source at bus2	0	0.2	$0.01 + j0$
DG at bus10	0.01	0.01	$3.76 + j6.02$
DG at bus12	5.970	3.24	$0.06 + j0.02$
DG at bus19	10	10.21	$6.51 + j0$
Source at bus5	1.309	10.02	$5.42 + j2.78$
Source at bus8	1	2.94	$0.41 + j1.3$
Source at bus11	0	0	0
Source at bus13	0.05	0.01	$0.49 + j0.115$
Objective function F1	3.12	3.34	2.745
Sum of FCLs components sizes (p.u.)	21.4	18.64	27.07

Table 12 Δt of miscoordinated backup–main DOCR pairs under far-end fault in the meshed test system

DOCR pair	Near-end fault	Far-end fault	DOCR pair	Near-end fault	Far-end fault
19, 1	0.2954	−2.3440	6, 11	0.5459	0.0112
15, 2	0.3100	−0.0088	16, 11	0.2901	−0.0069
23, 2	0.5102	−0.0050	17, 19	0.3070	0.0244
15, 4	0.5624	0.0100	3, 21	0.3001	0.0119
19, 4	0.7613	0.0006	4, 21	0.6349	0.0256
23, 4	0.7568	0.0137	23, 21	1.0037	0.0394
9, 5	0.6116	−0.0281	4, 22	0.6743	0.0256
12, 5	0.5337	0.0006	11, 23	0.3162	−0.0050
8, 6	0.2882	−0.2114	4, 24	0.3154	−0.0050
12, 6	0.2606	0.1615	11, 24	0.3139	0.0038
8, 7	0.3190	−3.1842	24, 25	0.2974	0.0194
6, 8	1.1409	0.0056	24, 27	0.3392	0.0200
16, 8	1.3917	−0.0125	26, 28	0.3097	0.0113
5, 11	0.5393	0.0025	27, 28	0.3176	0.0106
			27, 29	0.2954	−0.4369

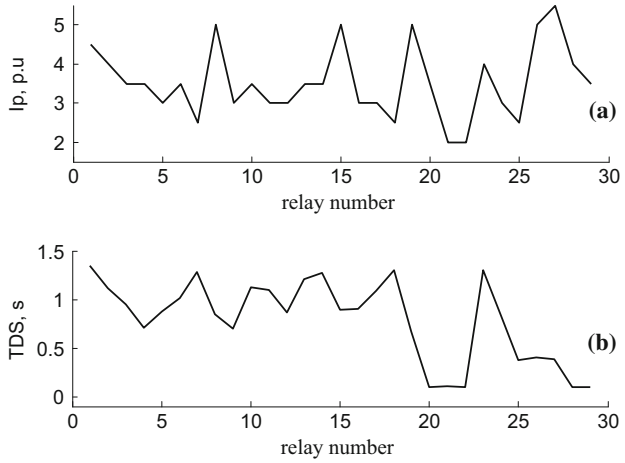

Fig. 15 Optimal settings of DOCRs in the meshed system considering both near-end and far-end faults. **a** The pickup current(I_p, p.u), **b** the time dial setting (TDS, s)

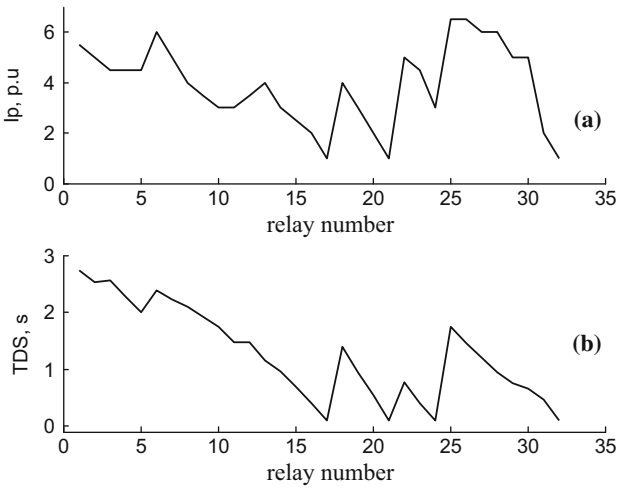

Fig. 17 Optimal settings of DOCRs in the radial system considering both near-end and far-end faults. **a** The pickup current (I_p, p.u), **b** the time dial setting (TDS, s)

(13)–(15) considering only single objective $F1$ in (11) using PSO. Results are given in Table 11 for X-FCL, R-FCL, and Z-FCL types. The choice of the proper FCL type depends on the LDC operators experience and FCL type's cost. The sum of FCLs components sizes is close to the case of considering only DOCRs for all FCL types.

5.4 Effect of Far-End Faults

For the meshed system, the DOCRs settings obtained in Sect. 5. A and shown in Fig. 4 considering only near-end faults are evaluated under far-end faults. It is found that

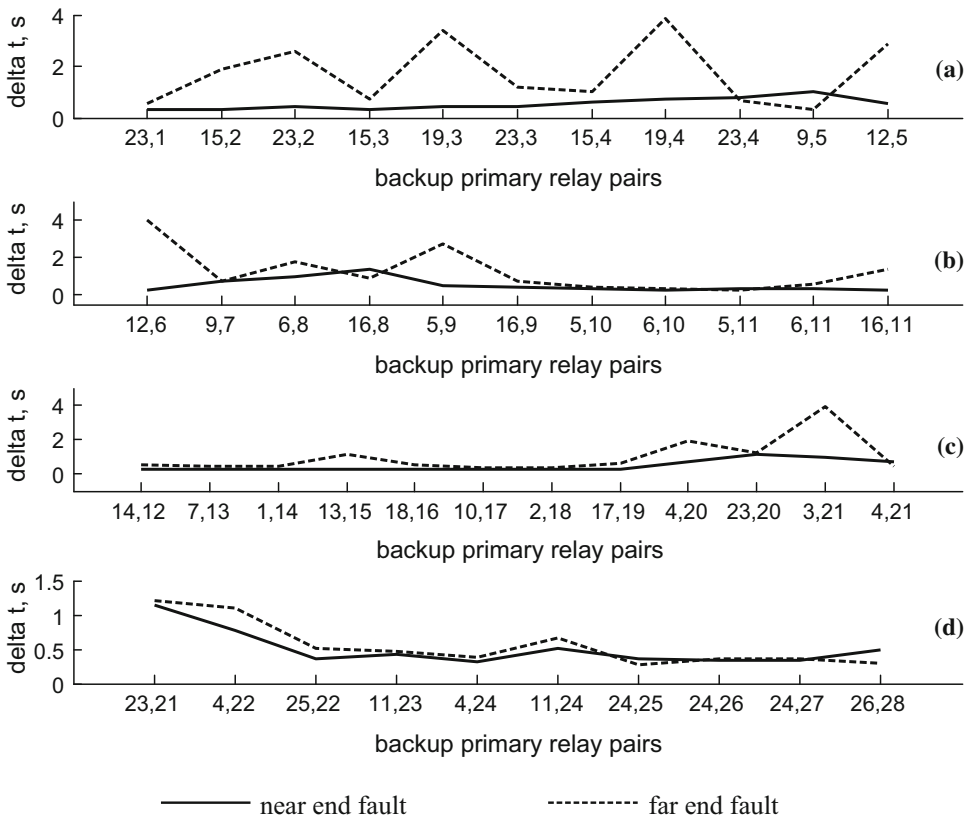

Fig. 16 Δt values of backup–main DOCR pairs in the meshed system considering both near-end and far-end faults

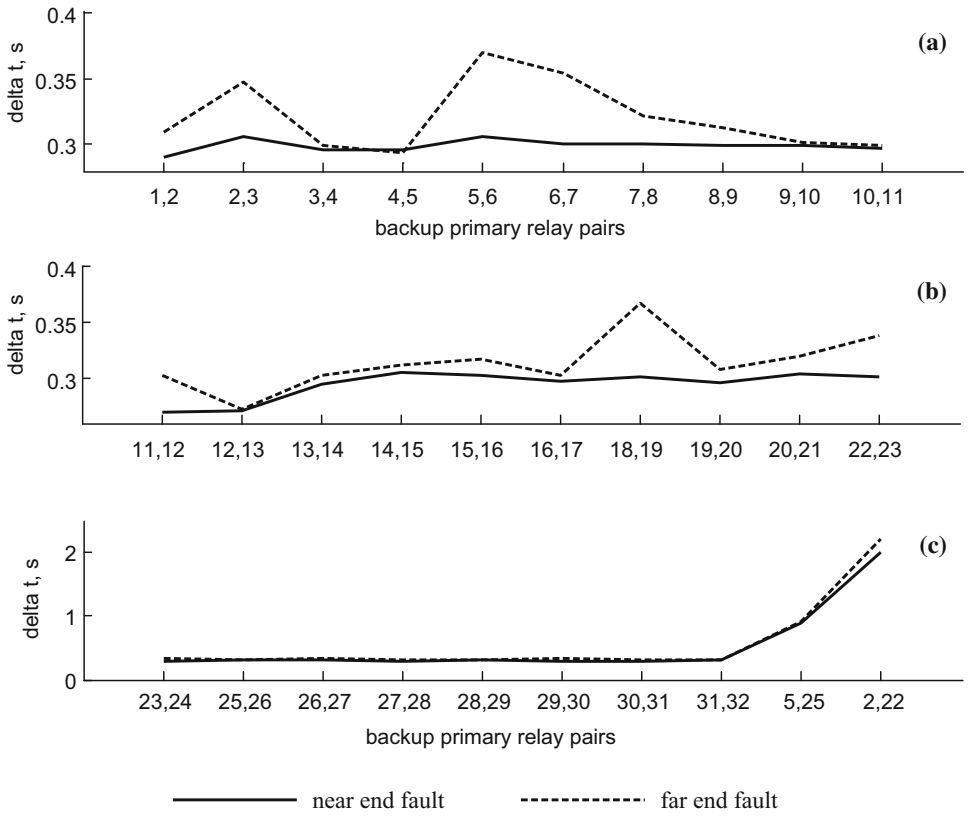

Fig. 18 Δt values of backup–main DOCR pairs in the radial system considering both near-end and far-end faults

some backup–main OCR pairs have violated coordination constraints as in Table 12. Hence, the OCRs coordination problem formulated in Sect. 2 is modified to include both near-end and far-end faults as in [30]. Then, the modified OCRs coordination problem is solved to get the new OCRs I_p and TDS settings as depicted in Fig. 15 for the meshed test system. All backup–main OCR pairs fulfill coordination constraints under both near-end and far-end faults. Δt is greater than 0.27 s for all backup–main OCR pairs as shown in Fig. 16. Besides, the far-end faults are considered also in the DOCRs setting problem for the radial test system in Fig. 3. The results are demonstrated in Figs. 17 and 18, which are the counterparts of Figs. 15 and 16, respectively.

6 Conclusion

The paper is focused on maintaining the directional OCRs coordinated operation in PDS with DGs. Application of FCLs is adopted as an effective solution that would save any need to OCRs resetting. Optimal locations and sizes of FCLs are searched to accomplish OCRs coordination at minimum cost of prospective FCLs. Therefore, the FCLs location and sizing problem is formulated as a constrained multi-objective optimization problem. BMOP coordination index and the sum of FCLs components sizes are considered as the two objectives to be minimized. The proposed algorithm is applied to meshed and radial power systems at different DGs arrangements using different types of FCLs. Furthermore, the OCRs coordination problem is studied when the system includes both directional and non-directional OCRs. Results show that:

- Optimal installation of FCLs maintains coordination of all BMOP.
- Multi-objective optimization results in drastically less sum of FCLs components sizes than using only BMOP coordination index as the only objective. This is noticed for all DG conditions, for all FCLs types and for both study systems.
- There is no much difference in the sum of FCLs components sizes for the resistive, inductive, and compound FCL types. However, resistive FCL type achieves markedly better value for BMOP coordination index.
- The sum of FCLs components sizes of the radial PDS is much bigger than the meshed PDS.

References

1. Hemmati, S; Sadeh, J: Applying superconductive fault current limiter to minimize the impacts of distributed generation on the

distribution protection systems, in 11th International Conference on Environment and Electrical Engineering (EEEIC), pp. 808-813, (2012)
2. Khan, U.: Impact of distributed generation on electrical power network. www.wppt.pwr.wroc.pl.
3. Noghabi, A; Mashhadi, H; Sadeh, J: Optimal coordination of directional overcurrent relays considering different network topologies using interval linear programming. IEEE Trans. Power Deliv. **25**(3), 1348–1354 (2010)
4. Abdelaziz, A.Y.; Talaat, H.E.A.; Nosseir, A.I.; Hajjar, A.A.: An adaptive protection scheme for optimal coordination of overcurrent relays. Electr. Power Syst. Res. **61**, 1–9 (2002)
5. Knable, A.H.: A standardised approach to relay coordination, in Proceedings of IEEE Power Engineering Society Winter Meeting, New York, pp. 58–62, (1969)
6. Dwaraknath, M.H.; Nowitz, L.: An application of linear graph theory for co-ordination of directional overcurrent relays. in Proceedings of SIAM Conference on Electric Power Problems: Mathematical Challenge, Seattle, pp. 104–114, (1980)
7. Damborg, M.J., et al.: Computer aided transmission protection system design, part I: algorithm. IEEE Trans. Power Appar. Syst. **103**(1), 51–59 (1984)
8. Urdaneta, A.J.; Restrepo, H.; Marquez, S.; Sanchez, J.: Coordination of directional overcurrent relay timing using linear programming. IEEE Trans. Power Deliv. **11**(1), 112–129 (1996)
9. Abyaneh, H.A.; Al-Dabbagh, M.; Karegar, H.K.; Sadeghi, S.H.; Khan R., A.: A new optimal approach for coordination of overcurrent relays in interconnected power systems. IEEE Trans. Power Deliv. **18**(2), 430–435 (2003)
10. So, C.W.; Li, K.K.; Lai, K.T.; Fung, K.Y.: Application of genetic algorithm to overcurrent relay grading coordination, in Proceedings of 6th International Conference Developments in Power System Protection, pp. 60–69, (1997)
11. Jager, J.; Shang, L.: High-impedance protection applications for tripping acceleration in networks with DG, in Transmission and Distribution Conference and Exhibition, pp. 1–5, (2005)
12. Javadian, S.A.; Haghifam, M.-R.: Protection of distribution networks in presence of DG using distribution automation system capabilities, in IEEE Power and Energy Society General Meeting, pp. 1–6, (2008)
13. Sortomme, E.; Venkata, S.S.; Mitra, J.: Microgrid protection using communication-assisted digital relays. IEEE Trans. Power Deliv. **25**(4), 2739–2796 (2010)
14. Ye, L.; Majoros, M.; Coombs, T.; Campbell, A.M.: System studies of the superconducting fault current limiter in electrical distribution grid. IEEE Trans. Appl. Supercond. **17**, 2339–2342 (2007)
15. Cakal, G.; Bagriyanik, F.; Bagriyanik, M.: The effect of fault current limiters on distribution systems with wind turbine generators. Int. J. Renew. Energy Res. **3**(1), 149–154 (2013)
16. Shahriari, S.; Yazdian, A.; Haghifam, M.: Fault current limiter allocation and sizing in distribution system in presence of distributed generation, in IEEE Power & Energy Society General Meeting, pp. 1–6, (2009)
17. Zeineldin, H.H.; Xiao, W.: Optimal fault current limiter sizing for distribution systems with DG, in IEEE Power and Energy Society General Meeting. pp. 1–5 (2011)
18. El-Khattam, W.; Sidhu, T.S.: Restoration of directional overcurrent relay coordination in distributed generation systems utilizing fault current limiter. IEEE Trans. Power Deliv. **23**(2), 576–585 (2008)
19. Reyes-Sierra, M.; Coello, C.: Multi-objective particle swarm optimizers: a survey of the state-of-the-art. Int. J. Comput. Intell. Res. **2**(3), 287–308 (2006)
20. Tang G.; Iravani M.R.: Application of a fault current limiter to minimize distributed generation impact on coordinated relay protection, in Presented at the International Conference on Power Systems Transients IPST'05, Montreal, Canada, June 19–23, (2005)
21. Payam, MS; Bijami, E; Abdollahi, M; Dehkordi, AS: Optimal coordination of directional overcurrent relay for power delivery system with a hybrid shuffled frog leaping algorithm. Aust. J. Basic Appl. Sci. **5**(12), 1949–1957 (2011)
22. Park, J.-B.; Lee, K.-S.; Shin, J.-R.; Lee, K.: A particle swarm optimization for economic dispatch with nonsmooth cost functions. IEEE Trans. Power Syst. **20**(1), 34–42 (2005)
23. Abido, M.: Two-level of nondominated solutions approach to multiobjective particle swarm optimization, in GECCO'07, London, England, July 7–11, (2007)
24. Reddy, M.; Kumar, D.: Multi-objective particle swarm optimization for generating optimal trade-offs in reservoir operation. Hydrol. Process. **21**, 2897–2909 (2007)
25. Univ. Washington. Seattle. http://www.ee.washington.edu/research/pstca/. (Mar. 2006)
26. Venkatesh, B.; Ranjan, R.; Gooi, H.B.: Optimal reconfiguration of radial distribution systems to maximize loadability. IEEE Trans. Power Syst. **19**(1), 260–266 (2004)
27. IEEE standard, inverse-time characteristic equations for overcurrent relays, IEEE Std. C37.112-1996
28. Aslinezhad, M.H.; Sadeghzadeh, S.M.; Olamaei, J.: Overcurrent relays coordination in distribution systems in presence of distributed generation. IJTPE **3**(2), 40–46 (2011)
29. Brooke, A.; Kendrick, D.; Meeraus, A.: GAMS: a user's guide. Scientific, San Francisco (1988)
30. Yang, M.-T.; Liu, A.: Applying hybrid PSO to optimize directional overcurrent relay coordination in variable network topologies. J. Appl. Math. **2013**, 1–9 (2013)